Supplemental Material

Bulletin of the American Meteorological Society
Tropical Cyclone Precipitation, Infrared, Microwave, and Environmental Dataset (TC PRIMED)
https://doi.org/10.1175/BAMS-D-21-0052.2

Tropical Cyclone Precipitation, Infrared, Microwave, and Environmental Dataset (TC PRIMED): A Summary of Previous Work

Muhammad Naufal Razin, Christopher J. Slocum, John A. Knaff, Paula J. Brown, and Michael M. Bell

We present below a list of public and private datasets of satellite passive microwave observations of tropical cyclones that were compiled before TC PRIMED. We acknowledge that other datasets of tropical cyclone observations exist, such as those in the infrared and sounding channels, that are publicly available and/or were used for notable research. However, since TC PRIMED centers around passive microwave imagery — with supplemental infrared imagery and model outputs and diagnostics — we focus on existing passive microwave datasets. We begin with the public datasets.

1. The Naval Research Laboratory's Tropical Cyclone website (NRL TC; https://www.nrlmry.navy.mil/TC.html) is one of the main sources for near real-time passive microwave imagery of tropical cyclones around the globe (Hawkins et al. 2001). The website provides tropical cyclone observations from sensors such as the AMSR2, AMSR-E, AMSUB, GMI, TMI, SSM/I, and SSMIS — with operationally-useful imagery that include the 37 and 85–92 GHz brightness temperatures and derived products (i.e., the 37 GHz color composite), retrieved surface precipitation rate and surface winds, microwave-based total precipitable water, and coincident observations in the visible, infrared and water vapor channels from other geostationary or low-Earth orbit sensors. Their extensive archive of global tropical cyclone imagery spans from 1997 to present.

2. The Cooperative Institute for Meteorological Satellite Studies (CIMSS) at the University of Wisconsin-Madison also provides near real-time satellite imagery of tropical cyclones across the globe through their website (http://tropic.ssec.wisc.edu/tropic.php). Their website allows users to display tropical cyclone satellite imagery in the infrared, visible and water vapor channels, as well as passive microwave brightness temperature observations in the atmospheric temperature channels of the AMSU sensors and in the high frequency channels (85–89 GHz) when available. Users can also overlay other near real-time products such as sea surface temperatures, microwave-based total precipitable water, and satellite-derived products such as atmospheric motion vectors, vertical shear, low-level convergence, upper-level divergence, vorticity and deep-layer motion vectors. The length of their archive varies depending on the type of product.

3. The Regional and Mesoscale Meteorology Branch (RAMMB) of NOAA/NESDIS, collocated at the Cooperative Institute for Research in the Atmosphere (CIRA), runs a website that displays near real-time products (TC Real-Time; https://rammb-

data.cira.colostate.edu/tc_realtime/) for tropical cyclones across the globe. The products include raw and derived satellite products like the infrared, water vapor, visible and natural color imagery from geostationary or low-Earth orbit satellites, high-frequency (85–89 Hz) passive microwave imagery when available, microwave-based total precipitable water, multi-platform surface wind analysis, and satellite-based wind radii estimates. The website also provides select near real-time model data such as precipitation, sea surface temperature, vorticity, vertical motion, 10-m wind speed and sea level pressure, along with intensity guidance and experimental wind speed probabilities. While their data archive begins in the 2006 tropical cyclone season, data availability since 2006 depends on the type of product.

4. Remote Sensing Systems (RSS) also runs a website of near real-time satellite products for global tropical cyclones (https://www.remss.com/tropical-cyclones/storm-watch/). They specialize in satellite-based surface wind vectors, sea surface temperatures, and surface rain rate. Their archive spans from 1999 to present.

5. NASA's Jet Propulsion Laboratory (JPL) developed the Tropical Cyclone Information System (TCIS; https://tropicalcyclone.jpl.nasa.gov/) to provide users with a framework that incorporates model forecasts with satellite and airborne observations (Hristova-Veleva et al. 2020). The two branches of TCIS that are relevant in the context of performing tropical cyclone analysis using satellite observations and model outputs are the North Atlantic Hurricane Watch (NAHW) and the Tropical Cyclone Data Archive (TCDA). The NAHW is an interactive portal that allows users to interrogate and perform some online analyses on satellite observations and select model outputs of tropical cyclones in the North Atlantic and Eastern Pacific basins. Through this interactive portal, users can analyze tropical cyclone structure and environment, as well as compare model forecasts with observations. Data from NAHW spans from 2012 to present. Meanwhile, the TCDA contains multi-platform satellite imagery and corresponding digital data files of tropical cyclones throughout the globe. Users can browse the imagery of satellite observations before opting to download their respective digital data files. TCDA data spans from 1999 to 2010, with plans to include digital data up to the most recent tropical cyclone season.

6. The JAXA Earth Observation Research Center (EORC) runs a website that provides near real-time imagery of tropical cyclones throughout the globe from select few sensors such as the TRMM MI, TRMM PR, GPM MI, GPM DPR, AMSR, AMSR2, and AMSR-E (https://sharaku.eorc.jaxa.jp/TYP_DB/index_e.html). Users can also download archive digital data that spans from the date that the satellite became operational to the present or the date that the satellite was decommissioned. Depending on the sensor, users can access satellite observations that include brightness temperature data, precipitation data, total precipitable water data, or surface wind data.

7. The HURSAT-MW dataset consists of passive microwave brightness temperature observations of tropical cyclones throughout the globe from the SSM/I sensor (Knapp 2008; https://www.ncdc.noaa.gov/hursat/index.php?name=hursat-mw). HURSAT-MW spans the period from 1987 to 2009, and consists of SSM/I data in standard swath format and gridded format.

8. Jiang et al. (2011) developed a TRMM-based Tropical Cyclone Precipitation Feature database (TCPF; http://atmos.tamucc.edu/trmm/) that spans the whole period the TRMM satellite was operational (1998–2014). The TCPF database consists of observations from all of the TRMM sensors (VIRS, TMI, PR, and LIS), a multi-satellite rainfall product (TRMM 3B42), NCEP reanalysis, and basic tropical cyclone information such storm motion vector and magnitude and future 12-, 24-, 36- and 48-hour intensity changes. TCPF offers data in multiple data levels, from the pixel properties (Level 1), identified precipitation features (Level 2), and gridded precipitation feature statistics (Level 3).

TC PRIMED addresses some of the drawbacks from these datasets, such as:

- Some of the public datasets are image files of satellite observations. These image files do not give users a lot of flexibility to interrogate the data. TC PRIMED contains digital files that users can digitally read and interrogate using a programming language.
- Digital files of satellite observations from some of these datasets are limited to certain sensors and time periods, and contain uncalibrated passive microwave brightness temperatures. TC PRIMED contains observations from multiple sensors in the GPM constellation, spans a long time period from 1998–2019 with potential for updates to include observations from 1987 up to the most recent tropical cyclone season, and contains inter-calibrated microwave brightness temperature data.
- A majority of the public datasets do not have supplemental model analyses and derived products. Those that have model products have limited model outputs and/or inconsistent periods of model availability. TC PRIMED provides model reanalysis outputs and derived products from a single, consistent source throughout the lifetime of each tropical cyclone in the dataset, and includes all of the variables typically used to diagnose the tropical cyclone environment.

Relative to these public datasets, TC PRIMED falls short in some respects in that:

- It is not built for near real-time analysis.
- It does not contain sounder data.
- It does not contain environmental data derived from satellite observations such as atmospheric temperature and humidity profiles, surface wind profiles, and sea surface temperatures.

- It does not have an interactive online portal that allows users to perform online analysis or display and overlay various variables online before downloading the data.

There are numerous tropical cyclone analyses in published literature that used the public datasets discussed above. However, in addition to the public datasets discussed above, there are researchers that have performed tropical cyclone analyses in published literature using their own dataset of satellite passive microwave observations of tropical cyclones. We list these articles below. This list is non-exhaustive, as there are likely other datasets that we may have missed in our review of the literature. Given the private nature of these datasets, retracing the data origin and subsequent processing information was difficult. Therefore, we group these published literature based on the similarity of their datasets or analyses.

A few studies have analyzed brightness temperature observations and microwave-derived precipitation rates from SSM/I relative to tropical cyclone intensity and/or future intensity change (Rao and MacArthur 1994, Rodgers et al. 1994, Rodgers and Pierce 1995, Rao and McCoy 1997, Cecil and Zipser 1999). The dataset of SSM/I observations utilized in each of these studies covers different tropical cyclone basins and/or periods. Cecil and Zipser (1999) also included lightning observations from the optical transient detector aboard a separate low-Earth orbiting satellite. Meanwhile, Rodgers et al. (2000) analyzed the fractional contribution of tropical cyclone precipitation to the North Pacific basin using SSM/I-derived precipitation rates.

Cecil et al. (2002) analyzed the characteristics of tropical cyclone eyewalls and rainbands using the suite of sensors aboard the TRMM satellite, such as the precipitation radar (PR), microwave imager (MI), and lightning imaging sensor (LIS). Their dataset includes 261 TRMM overpasses of 45 tropical cyclones throughout the globe from 1997 through 1998. Lonfat et al. (2004) analyzed the distribution of precipitation in tropical cyclones using microwave-derived precipitation estimates from 2,121 TRMM overpasses of 260 tropical cyclones throughout the globe. Chen et al. (2006) analyzed the distribution of precipitation relative to the tropical cyclone motion vector and vertical shear vector. They used TRMM MI and PR data over the same period as in Lonfat et al. (2004).

In a similar effort, Cecil (2007) used microwave-derived precipitation estimates from SSM/I and TRMM to analyze the distribution of precipitation rates relative to the vertical shear vector, vertical shear magnitude, and sea surface temperatures. Their dataset contains observations of Atlantic tropical cyclones from 1988 to 2004. Wingo and Cecil (2010) also conducted an analysis of precipitation in tropical cyclones relative to the environmental vertical shear. Their dataset contains microwave-derived precipitation estimates from SSM/I, TRMM MI, and AMSR-E overpasses of global tropical cyclones from 1988 through 2002.

More recently, Yang et al. (2021) presented an updated climatology of the distribution of precipitation in tropical cyclones relative to the motion vector and vertical shear vector. Their dataset contains NASA's microwave-based precipitation estimates (Goddard Profiling algorithm; GPROF) from its constellation of sensors that observed tropical cyclones from 1998 through 2012. Instead of using data from individual overpasses, Guzman and Jiang (2021) used NASA's gridded multiplatform rainfall algorithm from 1998 through 2016 to show differences in azimuthal mean precipitation rates between different basins.

Using a dataset of SSM/I and TMI observations of Atlantic and eastern North Pacific tropical cyclones from 1995 to 2003, Jones et al. (2006) developed and tested a version of the statistical hurricane intensity prediction scheme (SHIPS) that incorporates predictors from passive microwave imagery observations. Similarly, Rozoff et al. (2015) examined an implementation of a probabilistic prediction model for tropical cyclone rapid intensification using predictors from passive microwave imagery. Their dataset consists of observations of Atlantic and eastern North Pacific tropical cyclones from the SSM/I, SSMIS, TRMM MI, and AMSR-E – covering a period from 1998 through 2012.

Using a dataset of SSM/I and TRMM observations of global tropical cyclones from 1987 through 2008, Harnos and Nesbitt (2011) analyzed the passive microwave convective signatures of tropical cyclones undergoing rapid intensification. Harnos and Nesbitt (2016) used SSM/I and TRMM observations of global tropical cyclones over the same period as in Harnos and Nesbitt (2011) to analyze the prevalence of different cloud types (e.g., deep convection, shallow cumuli, etc.) in tropical cyclones undergoing different future intensity change rates. Using passive microwave brightness temperatures as proxy for convective intensity and precipitation, Alvey et al. (2015) analyzed the distribution of the precipitation properties in tropical cyclones relative to different future intensity change rates. They used a multiplatform dataset that includes the TRMM MI, AMSR-E, SSM/I, and SSMIS observations of Atlantic and eastern North Pacific tropical cyclones from 1998 through 2012. Meanwhile, Leppert et al. (2013a, b) investigated tropical cyclogenesis in eastern North Pacific and eastern North Atlantic tropical easterly waves using the suite of sensors aboard the TRMM satellite (MI, PR, LIS) and a NASA dataset of infrared brightness temperature observations. Their dataset covers the period from 2001 through 2010.

Moreno (2015) used a dataset of imaging and sounding observations from AMSUA, SSMIS, and ATMS overpasses of Atlantic tropical cyclones from 2011 through 2013 to compare the performance of various tropical cyclone intensity estimation techniques. Xiang et al. (2019) used a multivariate linear regression technique to estimate tropical cyclone intensity using the Hai Yang 2A satellite's scatterometer data and SSMIS observations of tropical cyclones over the western North Pacific. Their dataset covers a period from 2012 through 2017. Similarly, Qian et al. (2020) used a stepwise regression method to estimate tropical cyclone intensity using global

passive microwave observations from the Fengyun-3B satellite. Their database covers a period from 2011 through 2016.

Cossuth (2014) developed microwave-based metrics to describe the tropical cyclone eye and eyewall characteristics. Wimmers et al. (2019) tested the utilization of a convolutional neural network on passive microwave observations to estimate tropical cyclone intensity. Yang et al. (2020) presented a climatology of passive microwave brightness temperatures in tropical cyclones relative to the motion vector and vertical shear vector. All three of these analyses used a dataset first documented in Cossuth (2014), which include passive microwave observations of tropical cyclones from 1987 through 2012 from SSM/I, SSMIS, TMI, AMSRE, and WindSat. To extract extra details from the lower-resolution SSM/I and SSMIS sensors, the dataset contains remapped SSM/I and SSMIS brightness temperature observations using the Backus-Gilbert approach (Poe 1990). In addition, the dataset uses inter-calibrated microwave brightness temperatures in the ice scattering channels, whereby all brightness temperatures in the 85 and 91 GHz frequencies were calibrated to match the brightness temperatures in the 89 GHz frequency (Yang et al. 2014). The dataset also includes outputs from an automated center tracking algorithm (ARCHER; Wimmers and Velden 2010, 2016).

As evident from the discussions above, passive microwave observations are indeed valuable in improving our understanding and forecast of tropical cyclones. However, in contrast to the private nature of the datasets above, TC PRIMED is a publicly-available dataset with well-documented data sources and processing information. Therefore, the larger scientific community can participate towards improving our understanding and forecast of tropical cyclones in a transparent manner and with openly reproducible results.

References

Alvey, III, G. R., J. Zawislak, and E. Zipser, 2015: Precipitation properties observed during tropical cyclone intensity change, *Mon. Wea. Rev.*, **143**, 4476–4492.

Cecil, D. J., 2007: Satellite-derived rain rates in vertically shear tropical cyclones. *Geophys. Res. Lett.*, **34**, L02811.

Cecil, D. J. and E. J. Zipser, 1999: Relationships between tropical cyclone intensity and satellite-based indicators of inner core convection: 85-GHz ice-scattering signature and lightning. *Mon. Wea. rev.*, **127**, 103–123.

Cecil, D. J., E. J. Zipser, and S. W. Nesbitt, 2002: Reflectivity, ice scattering, and lightning characteristics of hurricane eyewalls and rainbands. Part I: quantitative description. *Mon. Wea. Rev.*, **130**, 769–784.

Chen, S. S., J. A. Knaff, and F. D. Marks, Jr., 2006: Effects of vertical wind shear and storm motion on tropical cyclone rainfall asymmetries deduced from TRMM. *Mon. Wea. Rev.*, **134**, 3190–3208.

Cossuth, J. H., 2014: Exploring a comparative climatology of tropical cyclone core structures. Ph.D. dissertation, Dept. of Earth Ocean and Atmospheric Science, Florida State University, 185 pp, http://purl.flvc.org/fsu/fd/FSU_migr_etd-8965.

Guzman, O. and H. Jiang, 2021: Heavier inner-core rainfall of major hurricanes in the North Atlantic basin than in other global basins. *J. Clim.*, **34**, 5707–5721.

Harnos, D. S. and S. W. Nesbitt, 2011: Convective structure in rapidly intensifying tropical cyclones as depicted by passive microwave measurements. *Geophys. Res. Lett.*, **38**, L07805.

Harnos, D. S. and S. W. Nesbitt, 2016: Passive microwave quantification of tropical cyclone inner-core cloud populations relative to subsequent intensity change. *Mon. Wea. Rev.*, **144**, 4461–4482.

Hawkins, J. D., T. F. Lee, J. Turk, C. Sampson, J. Kent, and K. Richardson, 2001: Real-time internet distribution of satellite products for tropical cyclone reconnaissance. *Bull. Amer. Meteor. Soc.*, **82**, 567–578.

Hristova-Veleva and Coauthors, 2020: An eye on the storm: integrating a wealth of data for quickly advancing the physical understanding and forecasting of tropical cyclones. *Bull. Amer. Meteor. Soc.*, **101**, E1718–E1742.

Jiang, H., C. Liu, and E. J. Zipser, 2011: A TRMM-based tropical cyclone cloud and precipitation feature database. *J. Appl. Meteor. Climatol.*, **50**, 1255–1274.

Jones, T. A., D. Cecil, and M. DeMaria, 2006: Passive-microwave-enhanced statistical hurricane intensity prediction scheme. *Wea. Forecasting*, **21**, 613–635.

Knapp, K. R, Hurricane Satellite (HURSAT) data sets: Low Earth orbit infrared and microwave data, *28th AMS Conference on Hurricanes and Tropical Meteorology*, Orlando, FL, 28 April – 2 May, 2008.

Leppert, II, K. D., W. A. Petersen, and D. J. Cecil, 2013a: Electrically active convection in tropical easterly waves and implications for tropical cyclogenesis in the Atlantic and East Pacific. *Mon. Wea. Rev.*, **141**, 542–556.

Leppert, II, K. D., D. J. Cecil, and W. A. Petersen, 2013b: Relation between tropical easterly waves, convection, and tropical cyclogenesis: a Lagrangian perspective. *Mon. Wea. Rev.*, **141**, 2649–2668.

Lonfat, M., F. D. Marks, Jr., and S. S. Chen, 2004: Precipitation distribution in tropical cyclones using the Tropical Rainfall Measuring Mission (TRMM) Microwave Imager: a global perspective. *Mon. Wea. Rev.*, **132**, 1645–1660.

Moreno, D. C., 2015: Tropical cyclone intensity and position analysis using passive microwave imager and sounder data. M.S. thesis, Dept. of Engineering Physics, Air Force Institute of Technology, 93 pp, https://scholar.afit.edu/etd/89.

Poe, G., 1990: Optimum interpolation of imaging microwave radiometer data, *IEEE Trans. Geosci. Remote Sens*., **28**, 800–810.

Qian, B., H. Jiang, F. Weng, and Y. Wu, 2020: Climatology of passive microwave brightness temperatures in tropical cyclones and their relations to storm intensities as seen by FY-3B/MWRI. *Remote Sens.*, **12**, 147.

Rao, G. V. and P. D. MacArthur, 1994: The SSM/I estimated rainfall amounts of tropical cyclones and their potential in predicting the cyclone intensity changes. *Mon. Wea. Rev.*, **122**, 1568–1574.

Rao, G. V. and J. H. McCoy, 1997: SSM/I measure microwave brightness temperature (TB's), anomalies of TB's, and their relationship to typhoon intensification. *Nat. Hazards*, **15**, 1–19.

Rodgers, E. B., R. F. Adler, and H. F. Pierce, 2000: Contribution of tropical cyclones to the North Pacific climatological rainfall as observed from satellites. *J. Appl. Meteor.*, **39**, 1658–1678.

Rodgers, E. B., S. W. Chang, and H. F. Pierce, 1994: A satellite observational and numerical study of precipitation characteristics in western North Atlantic tropical cyclones. *J. Appl. Meteor.*, **33**, 129–139.

Rodgers, E. B. and H. F. Pierce, 1995: A satellite observational study of precipitation characteristics in western North Pacific tropical cyclones. *J. Appl. Meteor.*, **34**, 2587–2599.

Rozoff, C. M., C. S. Velden, J. Kaplan, J. P. Kossin, and A. J. Wimmers, 2015: Improvements in the probabilistic prediction of tropical cyclone rapid intensification with passive microwave observations. *Wea. Forecasting*, **30**, 1016–1038.

Wimmers, A. J., and C. S. Velden, 2010: Objectively determining the rotational center of tropical cyclones in passive microwave satellite imagery. *J. Appl. Meteor. Climatol.*, **49**, 2013–2034.

Wimmers, A. J., and C. S. Velden, 2016: Advancements in objective multisatellite tropical cyclone center fixing. *J. Appl. Meteor. Climatol.*, **55**, 197–212.

Wimmers, A., C. Velden, and J. H. Cossuth, 2019: Using deep learning to estimate tropical cyclone intensity from satellite passive microwave imagery. *Mon. Wea. Rev.*, **147**, 2261–2282.

Wingo, M. T. and D. J. Cecil, 2010: Effects of vertical wind shear on tropical cyclone precipitation. *Mon. Wea. Rev.*, **138**, 645–662.

Xiang, K., X. Yang, M. Zhang, Z. Li, and F. Kong, 2019: Objective estimation of tropical cyclone intensity from active and passive microwave remote sensing observations in the northwestern Pacific Ocean. *Remote Sens.*, **11**, 627.

Yang, S., R. Bankert, and J. Cossuth, 2020: Tropical cyclone climatology from satellite passive microwave measurements. *Remote Sens.*, **12**, 3610.

Yang, S., J. Hawkins, and K. Richardson, 2014: The improved NRL tropical cyclone monitoring system with a unified microwave brightness temperature calibration scheme. *Remote Sens.*, **6**, 4563–4581.

Yang, S., V. Lao, R. Bankert, T. R. Whitcomb, and J. Cossuth, 2021: Improved climatology of tropical cyclone precipitation from satellite passive microwave measurements. *J. Clim.*, **34**, 4521–4537.

Tropical Cyclone Precipitation, Infrared, Microwave, and Environmental Dataset (TC PRIMED): Data Source Documentation

Muhammad Naufal Razin, Christopher J. Slocum, John A. Knaff, Paula J. Brown, and Michael M. Bell

Inter-Calibrated Passive Microwave Brightness Temperatures

NASA Level 1C
Version 5

TC PRIMED uses inter-calibrated passive microwave brightness temperature observations from NASA's GPM constellation of low-Earth orbit (LEO) satellites. The GPM constellation consists of sensors from NASA's domestic and international partners, with the partnerships formed through bilateral agreements. The intercalibration process uses the GMI sensor aboard the GPM Core Observatory as a calibration standard for constellation sensors that have been in orbit long enough to allow for intercalibration. To simulate the different scan geometry of the different sensors, including the varying footprint sizes of cross-track scanning sounders, the intercalibration process uses radiative transfer models. TC PRIMED contains observations from sensors with enough channels to provide meaningful precipitation estimates.

The original files are stored locally at CSU/CIRA, allowing the TC PRIMED team to collocate the LEO observations with tropical cyclones. However, users can browse and download the non-tropical-cyclone-centric data from https://arthurhou.pps.eosdis.nasa.gov/. While TC PRIMED compiles the latest versions of the NASA products, users should be aware of the nuances of the different versions. Documentations on how specific versions differ from prior versions are presented here: https://arthurhou.pps.eosdis.nasa.gov/atbd.html.

Berg, W., and Coauthors, 2016: Intercalibration of the GPM microwave radiometer constellation. *J. Atmos. Oceanic Technol.*, **33**, 2639–2654, https://doi.org/10.1175/JTECH-D-16-0100.1.

NASA GSFC and GPM Intercalibration Working Group, 2017: Algorithm Theoretical Basis Document Version 1.8: NASA Global Precipitation Measurement (GPM) Level 1C Algorithms. NASA GSFC.

Sensor	Satellite	DOI
AMSR2	GCOM-W1	10.5067/GPM/AMSR2/GCOMW1/1C/05
AMSR-E	Aqua	10.5067/GPM/AMSRE/AQUA/1C/05
AMSU-B	NOAA-15	10.5067/GPM/AMSUB/NOAA15/1C/05
	NOAA-16	10.5067/GPM/AMSUB/NOAA16/1C/05
	NOAA-17	10.5067/GPM/AMSUB/NOAA17/1C/05

ATMS	Suomi-NPP	10.5067/GPM/ATMS/NPP/1C/05
	NOAA-20	10.5067/GPM/ATMS/NOAA20/1C/05
GMI	GPM	10.5067/GPM/GMI/R/1C/05
MHS	Metop-A	10.5067/GPM/MHS/METOPA/1C/05
	Metop-B	10.5067/GPM/MHS/METOPB/1C/05
	Metop-C	10.5067/GPM/MHS/METOPC/1C/05
	NOAA-18	10.5067/GPM/MHS/NOAA18/1C/05
	NOAA-19	10.5067/GPM/MHS/NOAA19/1C/05
SSM/I	DMSP-F11	10.5067/GPM/SSMI/F11/1C/05
	DMSP-F13	10.5067/GPM/SSMI/F13/1C/05
	DMSP-F14	10.5067/GPM/SSMI/F14/1C/05
	DMSP-F15	10.5067/GPM/SSMI/F15/1C/05
SSMIS	DMSP-F16	10.5067/GPM/SSMIS/F16/1C/05
	DMSP-F17	10.5067/GPM/SSMIS/F17/1C/05
	DMSP-F18	10.5067/GPM/SSMIS/F18/1C/05
	DMSP-F19	10.5067/GPM/SSMIS/F19/1C/05
TMI	TRMM	10.5067/GPM/TMI/TRMM/1C/05

NASA Goddard Profiling Algorithm (GPROF)
NASA Level 2A-CLIM
Version 5

Passive-microwave-based precipitation estimates in TC PRIMED come from NASA's Goddard Profiling Algorithm (GPROF). GPROF uses a Bayesian averaging method to weight the observed passive microwave brightness temperatures with an a-priori database of passive microwave brightness temperatures and precipitation information. The database comes from one year of global GPM observations — excluding observations over snow-covered surfaces — with the precipitation information coming from the GPM combined radar-radiometer algorithm averaged to the GMI footprint. For computational efficiency, GPROF separates the a-priori data based on surface types, total column water vapor, and 2-m temperature. To simulate the brightness temperature observations of the different constellation sensors, GPROF uses a radiative transfer model, producing a unique a-priori database for each sensor.

The original files are stored locally at CSU/CIRA, allowing the TC PRIMED team to collocate the LEO observations with tropical cyclones. However, users can browse and download the non-tropical-cyclone-centric data from https://arthurhou.pps.eosdis.nasa.gov/. While TC PRIMED compiles the latest versions of the NASA products, users should be aware of the nuances of the different versions. Documentations on how specific versions differ from prior versions are presented here: https://arthurhou.pps.eosdis.nasa.gov/atbd.html.

Kummerow, C. D., D. L. Randel, M. Kulie, N.-Y.Wang, R. Ferraro, S. J. Munchak, and V. Petkovic, 2015: The evolution of the Goddard profiling algorithm to a fully parametric scheme. *J. Atmos. Oceanic Technol.*, **32**, 165–176, https://doi.org/10.1175/JTECH-D-15-0039.1.

Passive Microwave Algorithm Team Facility, 2018: Algorithm Theoretical Basis Document: NASA Global Precipitation Measurement (GPM) GPROF2017 Version 1 and Version 2. NASA.

Sensor	Satellite	DOI
AMSR2	GCOM-W1	10.5067/GPM/AMSR2/GCOMW1/GPROFCLIM/2A/05
AMSR-E	Aqua	10.5067/GPM/AMSRE/AQUA/GPROFCLIM/2A/05
AMSU-B	NOAA-15	10.5067/GPM/AMSUB/NOAA15/GPROFCLIM/2A/05
	NOAA-16	10.5067/GPM/AMSUB/NOAA16/GPROFCLIM/2A/05
	NOAA-17	10.5067/GPM/AMSUB/NOAA17/GPROFCLIM/2A/05
ATMS	Suomi-NPP	10.5067/GPM/ATMS/NPP/GPROFCLIM/2A/05
	NOAA-20	10.5067/GPM/ATMS/NOAA20/GPROFCLIM/2A/05

GMI	GPM	10.5067/GPM/GMI/GPROFCLIM/2A/05
MHS	Metop-A	10.5067/GPM/MHS/METOPA/GPROFCLIM/2A/05
	Metop-B	10.5067/GPM/MHS/METOPB/GPROFCLIM/2A/05
	Metop-C	10.5067/GPM/MHS/METOPC/GPROFCLIM/2A/05
	NOAA-18	10.5067/GPM/MHS/NOAA18/GPROFCLIM/2A/05
	NOAA-19	10.5067/GPM/MHS/NOAA19/GPROFCLIM/2A/05
SSM/I	DMSP-F11	10.5067/GPM/SSMI/F11/GPROFCLIM/2A/05
	DMSP-F13	10.5067/GPM/SSMI/F13/GPROFCLIM/2A/05
	DMSP-F14	10.5067/GPM/SSMI/F14/GPROFCLIM/2A/05
	DMSP-F15	10.5067/GPM/SSMI/F15/GPROFCLIM/2A/05
SSMIS	DMSP-F16	10.5067/GPM/SSMIS/F16/GPROFCLIM/2A/05
	DMSP-F17	10.5067/GPM/SSMIS/F17/GPROFCLIM/2A/05
	DMSP-F18	10.5067/GPM/SSMIS/F18/GPROFCLIM/2A/05
	DMSP-F19	10.5067/GPM/SSMIS/F19/GPROFCLIM/2A/05
TMI	TRMM	10.5067/GPM/TMI/TRMM/GPROFCLIM/2A/05

GPM DPR and GMI Combined Precipitation
NASA Level 2B
Version 6

The GPM combined radar-radiometer algorithm produces precipitation profiles that best match both the DPR and GMI observations. However, observations such as radar reflectivity and precipitation type come solely from the DPR.

The original files are stored locally at CSU/CIRA, allowing the TC PRIMED team to collocate the LEO observations with tropical cyclones. However, users can browse and download the non-tropical-cyclone-centric data from https://arthurhou.pps.eosdis.nasa.gov/. While TC PRIMED compiles the latest versions of the NASA products, users should be aware of the nuances of the different versions. Documentations on how specific versions differ from prior versions are presented here: https://arthurhou.pps.eosdis.nasa.gov/atbd.html.

Olson, W. S. and GPM Combined Radar-Radiometer Algorithm Team, 2018: Algorithm Theoretical Basis Document: GPM Combined Radar Radiometer Precipitation Version 5. NASA.
DOI: 10.5067/GPM/DPRGMI/CMB/2B/06

TRMM PR and TMI Combined Precipitation
NASA Level 2B
Version 6

The TRMM combined radar-radiometer algorithm is similar to its GPM counterpart, except that it generates precipitation profiles that best match the PR and TMI observations. Similarly, observations such as radar reflectivity and precipitation type come solely from the PR.

The original files are stored locally at CSU/CIRA, allowing the TC PRIMED team to collocate the LEO observations with tropical cyclones. However, users can browse and download the non-tropical-cyclone-centric data from https://arthurhou.pps.eosdis.nasa.gov/. While TC PRIMED compiles the latest versions of the NASA products, users should be aware of the nuances of the different versions. Documentations on how specific versions differ from prior versions are presented here: https://arthurhou.pps.eosdis.nasa.gov/atbd.html.

DOI: 10.5067/GPM/PRTMI/TRMM/2B/06

RAMMB/CIRA Tropical Cyclone IR Archive

NOAA Level 2

The RAMMB/CIRA Tropical Cyclone IR archive contains infrared observations of global tropical cyclones starting from 2005. However, it contains observations of all Atlantic tropical cyclones in GOES-E or GOES-W views going back to 1982, and East Pacific tropical cyclones back to about 1987. The spatial resolution of the RAMMB/CIRA infrared data is 4 km. The temporal resolution is based on the availability from the geostationary satellites over the years and the location of the tropical cyclones. For instance, GMS/MTSAT data were typically half-hourly in the Northern Hemisphere, affecting West Pacific tropical cyclones, but hourly in the Southern Hemisphere. Whereas Meteosat-7 data were half-hourly in both hemispheres of the Indian Ocean. Meteosat-8–11 has a 15 minute resolution. The availability of GOES-E and GOES-W data depended more on storm location; that is, whether the storm is in the CONUS (15-minute), Northern Hemisphere (half-hourly) sectors, and whether rapid scan collection was occurring. Even then not all images are collected or pass quality control — resulting in varying time resolution. The following table lists the satellites from the RAMMB/CIRA archive included in TC PRIMED and their observation central wavelengths.

Satellite	Central Wavelength (μm)
FY-2C	11.2
GMS	11.2
GMS-5	11.2
GOES-8	10.7
GOES-9	10.7
GOES-10	10.7
GOES-11	10.7
GOES-12	10.7
GOES-13	10.7
GOES-14	10.7
GOES-15	10.7
GOES-16	10.3
GOES-17	10.3
Himawari-8	10.4, 11.2

Himawari-9	10.4
Meteosat-5	11.5
Meteosat-7	11.2
Meteosat-8 (MSG-1)	10.8
Meteosat-9 (MSG-2)	10.8
Meteosat-10 (MSG-3)	10.8
Meteosat-11 (MSG-4)	10.8
MTSAT-1R	10.8
MTSAT-2	10.8
NOAA-17	11.2

Hurricane Satellite Data (HURSAT) IR Archive
NOAA Level 2
Version 3

NCDC/NCEI collected the HURSAT data as part of the International Satellite Cloud Climatology Project (ISCCP). The HURSAT infrared data has a spatial resolution of 8 km and a temporal resolution of 3 hours. However, data gaps may exist due to bad data or data loss. The current version of HURSAT spans from 1978 to 2015. Since we prioritize the higher resolution IR data from the RAMMB/CIRA Tropical Cyclone IR archive, which began archiving global tropical cyclones in 2005, the number of HURSAT observations included in TC PRIMED after 2005 are limited. The following lists the satellites from the HURSAT archive included in TC PRIMED and their observation wavelength range.

Satellite	**Wavelength Range (μm)**
GMS-5	10.2 – 11.4
Meteosat-5	10.6 – 11.8
Meteosat-6	10.7 – 12.0

The HURSAT data used in TC PRIMED are stored locally at CIRA. However, users can browse and download this data from https://www.ncdc.noaa.gov/hursat/index.php?name=summary.

Knapp, K. R. and J. P. Kossin, 2007: New global tropical cyclone data from ISCCP B1 geostationary satellite observations. *Journal of Applied Remote Sensing*, **1**, 013505.

ECMWF Reanalysis Version 5 (ERA5)

NOAA Level 4

Version 5

To provide tropical cyclone environmental information, TC PRIMED uses the fifth-generation ECMWF reanalysis products (ERA5; Hersbach et al. 2020). ERA5 contains hourly analyzed fields at 0.25-degree horizontal grid spacing on single-level and pressure-level surfaces (Hersbach et al. 2018a,b). However, TC PRIMED provides select single- and pressure-level fields on their native grid at each synoptic time (00, 06, 12, 18 UTC) and within a 20° longitude × 20° latitude box centered on the tropical cyclone. The vertical resolution of the ERA5 fields in TC PRIMED includes the surface level, the 1000- to 100-hPa levels at every 50 hPa, and the 975- and 925-hPa levels.

The most commonly-used environmental diagnostics are the diagnostics calculated for the Statistical Hurricane Intensity Prediction Scheme (SHIPS). One version of SHIPS, the SHIPS Developmental Dataset, uses analyzed fields from the Climate Forecast System Reanalysis (CFSR) and the Global Forecast System (GFS) analyses for its calculation. Instead of using the CFSR and GFS fields, TC PRIMED uses the ERA5 fields to calculate the environmental diagnostics. For specific details on the diagnostics calculation, and the differences between the ERA5-derived environmental diagnostics and the SHIPS Developmental Dataset diagnostics, we refer readers to Slocum et al. (2022)

Users can browse and download the full suite of ERA5 data from https://cds.climate.copernicus.eu/.

Hersbach, H., and Coauthors, 2018: ERA5 hourly data on single levels from 1979 to present. Copernicus Climate Change Service (C3S) Climate Data Store (CDS). 10.24381/cds.adbb2d47

Hersbach, H., and Coauthors, 2018: ERA5 hourly data on pressure levels from 1979 to present. Copernicus Climate Change Service (C3S) Climate Data Store (CDS). 10.24381/cds.bd0915c6

Hersbach, H., and Coauthors, 2020: The ERA5 global reanalysis. *Quart. J. Roy. Meteor. Soc.*, **144**, 1999–2049, https://doi.org/10.1002/qj.3803.

Slocum, C. J., M. N. Razin, J. A. Knaff, and J. P. Stow, 2022: Does ERA5 mark a new era for resolving the tropical cyclone environment? *J. Climate*, **35**, 7147–7164, https://doi.org/10.1175/JCLI-D-22-0127.1.

TC PRIMED: Radius Scaling in Satellite Composites

Muhammad Naufal Razin, Christopher J. Slocum, John A. Knaff, Paula J. Brown, and Michael M. Bell

The scaling factor derives from Knaff et al. (2014), who created a uniform global tropical cyclone size metric that is applicable over a long period. The first step in their process is to obtain the azimuthal mean tangential wind speed at the 850 hPa level and 500 km radius (V500). To obtain V500, Knaff et al. (2014) first analyzed storm-centered infrared brightness temperatures from equidistant Cartesian grids onto cylindrical grids with a radial resolution of 4 km and an azimuthal resolution of 10 degrees. They used the variational analysis technique described in Mueller et al. (2006), but with filter half-power wavelengths of 10 km in radius and 22.5 degrees in azimuth. They then performed a principal component analysis on the azimuthal mean radial profiles of brightness temperatures, standardized at each radial bin. The first three principal components explain over 95% of the variance in their data.

Using multiple linear regression, they relate to V500 1) the first three principal components of the standardized azimuthal mean brightness temperatures and 2) the sine of the absolute latitude of the storm. To train their model, they used a catalog of V500 calculated for the Statistical Hurricane Intensity Prediction Scheme (SHIPS) and the Logistic Growth Equation Model (LGEM; DeMaria et al. 2005, DeMaria 2009). V500 comes from the operational GFS analysis and NCEP-NCAR reanalysis. The resulting equation for V500 is thus:

$$V500 = 2.488 + 11.478 \sin|\varphi| - (1.350 \times PC1) + (0.912 \times PC2) + (0.319 \times PC3)$$

Knaff et al. (2014) defines the size of the storm as the radius where the mean tangential wind speed is 5 knots at the 850 hPa level (R5), which they assumed to be essentially the same as the background flow. To obtain R5, they used V500 calculated for a particular tropical cyclone infrared observation and the mean values of R5, V500, and V1000 ($\underline{R5}$, V500c, and V1000c, respectively). V1000 is the azimuthal mean tangential wind speed at 1000 km radius. Similar to V500, Knaff et al. (2014) obtained V1000 from the average 850 hPa vorticity from r = 0 to r = 1000 km (ζ_{1000}) developed for SHIPS and LGEM, where $V1000 = (1000 \times \zeta_{1000}) / 2$. The resulting equation for R5 is thus:

$$R5 = \underline{R5} + (V500 - V500c)\frac{500}{(V500c - V1000c)}$$

Here, $\underline{R5}$ = 952 km, V500c = 5.05 m s^{-1}, and V1000c = 2.23 m s^{-1}. While the equation above provides R5 in units of km, R5 is usually converted to units of degrees latitude. However, R5

varies with tropical cyclone intensity. From Knaff et al. (2017), the following equation provides the intensity-based climatological values of R5:

$$R5c = 7.653 + \left(\frac{VM}{11.651}\right) - \left(\frac{VM}{59.076}\right)^2$$

Here, VM is the tropical cyclone intensity in units of knots and based on the Saffir-Simpson hurricane wind scale, while R5c is in units of degrees latitude.

To summarize, one can obtain V500 from a storm-centered infrared observation of a tropical cyclone. Using V500 and the mean values of R5, V500, and V1000 from Knaff et al. (2014), one can then obtain the R5 of the storm at the time of the infrared observation. However, the climatological value of R5 (R5c) depends on the intensity of the tropical cyclone.

The scaling factor (F_{R5}) scales the observation radii based on the observed value of R5 relative to the global intensity-based climatological value of R5 (R5c), where:

$$F_{R5} = \frac{R5}{R5c}$$

Subsequently, one can obtain the scaled radius (R*) by dividing the observed/physical radius (r) by the scaling factor, such that

$$R^* = \frac{r}{F_{R5}}$$

Note that if the observed tropical cyclone is smaller than climatology for its intensity (R5 < R5c), $F_{R5} < 1$ and subsequently, R* > r. Therefore, the radius scaling serves to expand the observation radius and enlarge the observation projection for analysis. The reverse is true for tropical cyclones that are bigger than climatology for its intensity (R5 > R5c). We provide examples from Hurricane Michael (2012) and Typhoon Bolaven (2012) below. Hurricane Michael was marginally smaller than its intensity-based climatology at the observation time while Typhoon Bolaven was bigger than its intensity-based climatology at the observation time.

CIRA calculates and archives three-hourly R5 values for each tropical cyclone locally. In scaling the radius for our TC PRIMED composites, we linearly interpolate the three-hourly R5 values to the observation time and obtain R5c using the equation above and the best-track tropical cyclone intensity interpolated to the observation time. The respective minimum, maximum, and median values of F_{R5} in the composites are 0.14, 1.92, and 0.99.

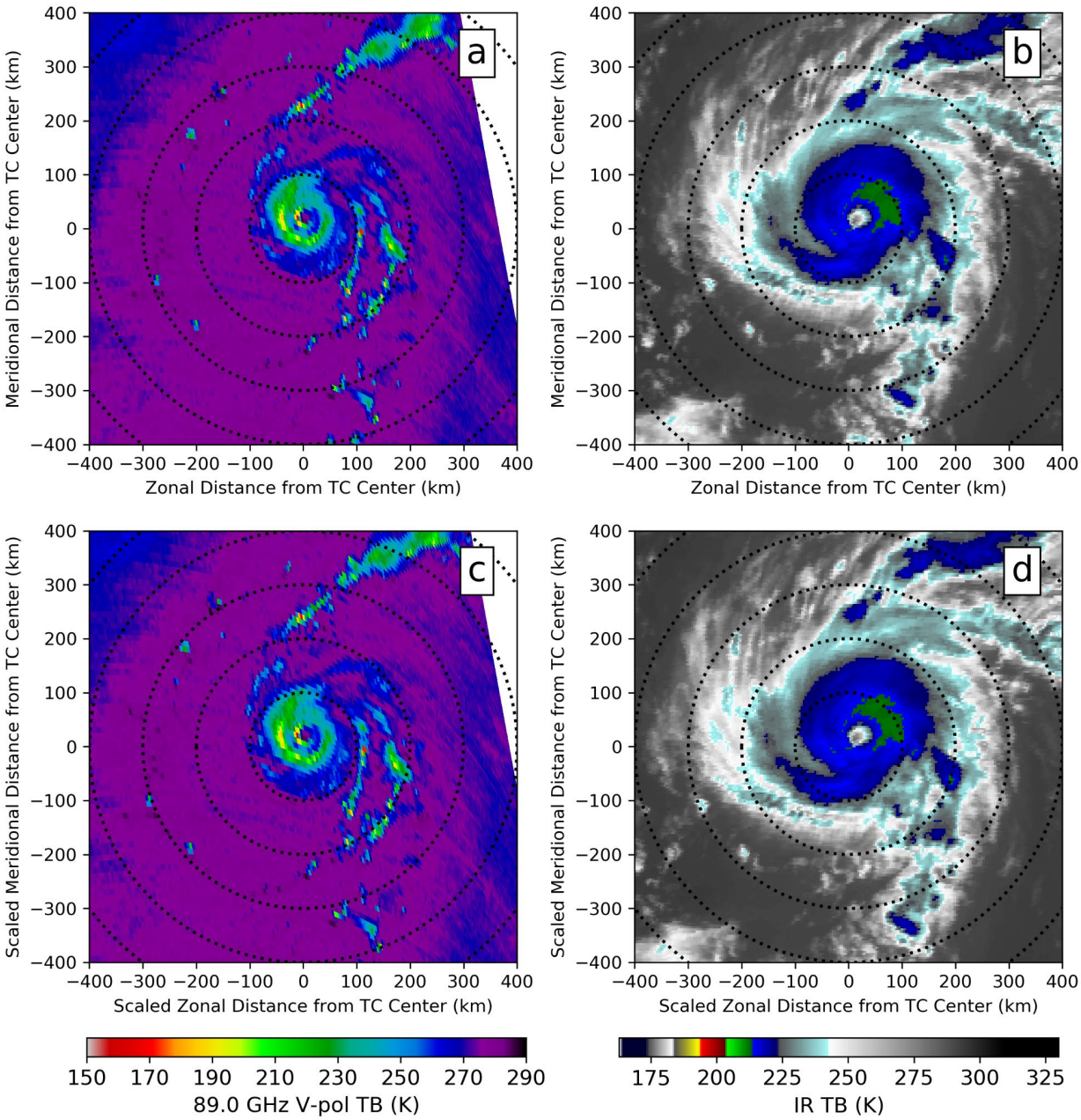

Observation of Hurricane Michael (2012) from TC PRIMED in the vertically polarized 89.0 GHz channel (left columns) from AMSR2 on September 6th at 10:13:06 UTC and in the 10.7 micron infrared channel (right columns) from GOES-13 on September 6th at 10:15:00 UTC. The top panels show unscaled observations and the bottom panels show scaled observations, with the scaling factor F_{R5} of 0.95 (a storm that is marginally smaller than its intensity-based climatology). Intensity at the time of the observation, interpolated from best-track, is 96 knots.

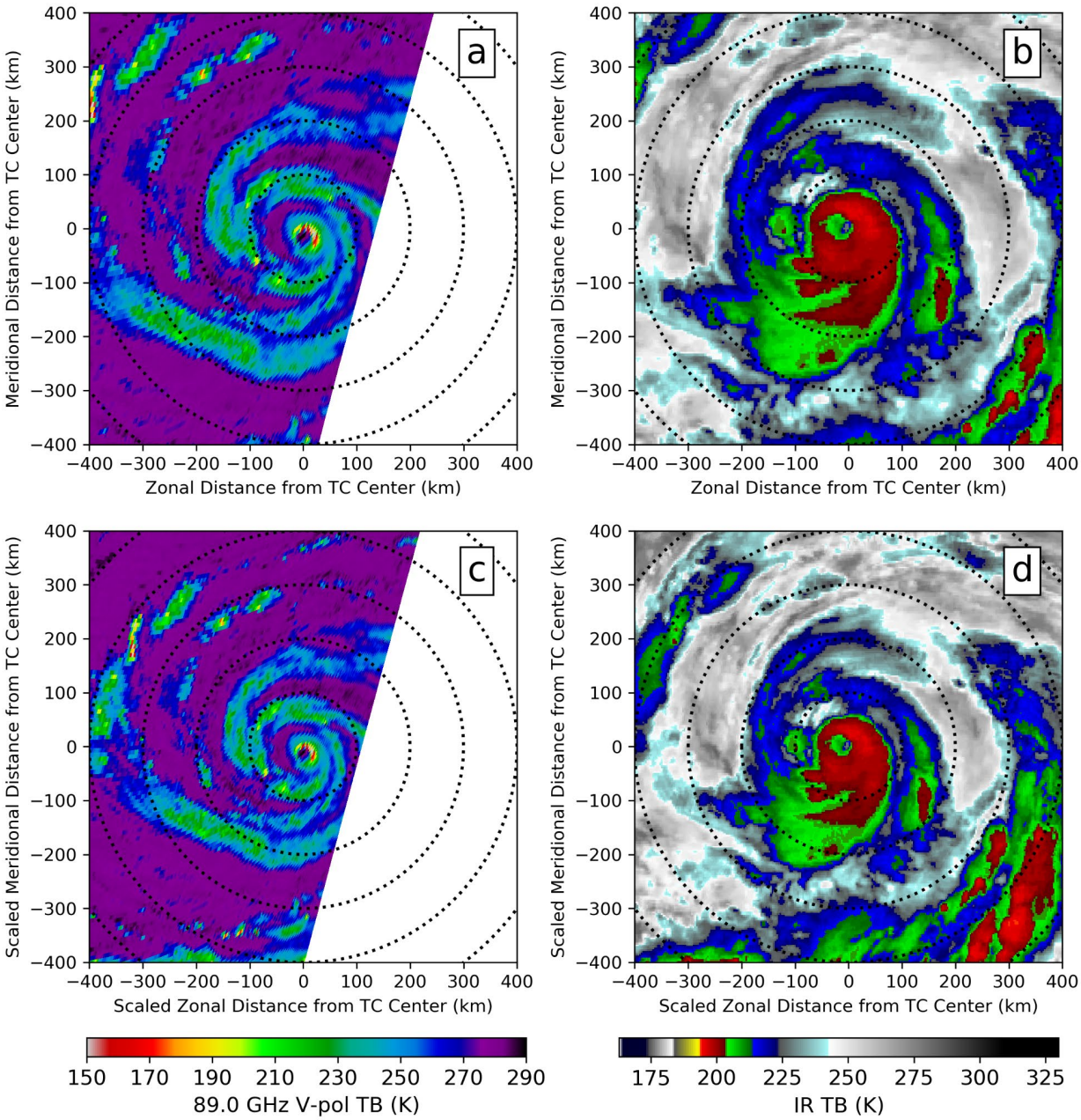

Observation of Typhoon Bolaven (2012) from TC PRIMED in the vertically polarized 89.0 GHz channel (left columns) from AMSR2 on August 24th at 11:19:24 UTC and in the 10.8 micron infrared channel (right columns) from MTSAT-2 on August 24th at 11:14:00 UTC. The top panels show unscaled observations and the bottom panels show scaled observations, with the scaling factor F_{R5} of 1.2 (a storm that is bigger than its intensity-based climatology). Intensity at the time of the observation, interpolated from best-track, is 124 knots.

References

DeMaria, M., M. Mainelli, L. K. Shay, J. A. Knaff, and J. Kaplan, 2005: Further improvements to the statistical hurricane intensity prediction scheme SHIPS. *Wea. Forecasting*, **20**, 531–543, https://doi.org/10.1175/WAF862.1.

DeMaria, 2009: A Simplified Dynamical System for Tropical Cyclone Intensity Prediction. *Mon. Wea. Rev.*, **137**, 68–82, https://doi.org/10.1175/2008MWR2513.1.

Knaff, J. A., S. P. Longmore, and D. A. Molenar, 2014: An objective satellite-based tropical cyclone size climatology. *J. Climate*, **27**, 455–476, https://doi.org/10.1175/JCLI-D-13-00096.1.

Knaff, J. A., C. R. Sampson, and G. Chirokova, 2017: A global statistical-dynamical tropical cyclone wind radii forecast scheme. *Wea. Forecasting*, **32**, 629–644, https://doi.org/10.1175/WAF-D-16-0168.1.

Mueller, K. J., M. DeMaria, J. A. Knaff, J. P. Kossin, and T. H. Vonder Haar, 2006: Objective estimation of tropical cyclone wind structure from infrared satellite data. *Wea. Forecasting*, **21**, 990–1005.